

# Cost-Effective Monitoring of the Fuel Air Equivalence-Ratio with a Lambda Sensor and a Microcontroller in a Downdraft Biomass Gasifier

Jean Fidele Nzihou, Salou Hamidou, Ousmane Zoundi, Frederic Ouattara, Bila Gerard Segda

Formation and Research Unit in Sciences and Technologies, University Norbert ZONGO, Koudougou, Burkina Faso

Email: [jfnzihou@edilf.fr](mailto:jfnzihou@edilf.fr)

**How to cite this paper:** Nzihou, J.F., Hamidou, S., Zoundi, O., Ouattara, F. and Segda, B.G. (2024) Cost-Effective Monitoring of the Fuel Air Equivalence-Ratio with a Lambda Sensor and a Microcontroller in a Downdraft Biomass Gasifier. *Open Journal of Applied Sciences*, 14, 545-560.  
<https://doi.org/10.4236/ojapps.2024.142039>

**Received:** January 22, 2024

**Accepted:** February 26, 2024

**Published:** February 29, 2024

Copyright © 2024 by author(s) and Scientific Research Publishing Inc.

This work is licensed under the Creative Commons Attribution International License (CC BY 4.0).

<http://creativecommons.org/licenses/by/4.0/>



Open Access

## Abstract

The operation of biomass treatment devices such as gasifiers is based on the control of key parameters that play an important role in product formation. These include: temperature, excess oxygen, relative humidity and biomass composition. This work focuses on excess oxygen and temperature. Unfortunately, flue gas oxygen analyzers are expensive and not accessible to small industries. However, the equivalence ratio is linked to excess oxygen and has the advantage of not depending on biomass composition. This study therefore focuses on the design and development of a device for controlling this equivalence ratio by measuring oxygen concentration using a self-propelled Lambda probe, and a system for monitoring this equivalence ratio using an Arduino Uno 3 microcontroller. The temperature is recorded with an accuracy of  $\pm 1.5^{\circ}\text{C}$ . For a heating time of 10 minutes, the response time to temperature change is around 3 seconds, which is sufficient for the device to function properly. This simple device is an efficient and cost-effective means of checking the equivalence ratio.

## Keywords

Equivalence Ratio, Biomass, Gasification, Lambda Sensor, Microcontroller, C++

## 1. Introduction

Biomass gasification is used very little in Burkina Faso, although it has proven to be one of the most efficient methods for converting biomass into thermal and electrical energy. Despite the abundance of waste of agricultural, plant and

household origin, the large-scale recovery of this conversion process is very little developed in Burkina Faso [1] [2].

In a review article published in 2014, gasification of waste was found as an interesting alternative to waste dumping in landfills through thermal valorization in Burkina-Faso [3]. Other studies on the development of biomass energy in Africa agree with the main conclusions of that review [4] [5] [6].

In gaseous combustion like gasoline, quantity of air is usually greater than of combustible for energy saving considerations. Therefore, Air-Fuel Ratio (AFR) is used to calculate the equivalence ratio [7] [8] [9].

However, in the biomass gasification, the aim is to produce combustible gases like carbon monoxide (CO) and hydrogen (H<sub>2</sub>) that result from incomplete combustion of the biomass feed [10] [11]. Detailed explanation will be given in section “2.2.3 Determination of the Equivalence Ratio”. For now, we will consider AFR when talking about combustion and FAR when talking about gasification.

Commercial Lambda sensors used in the automotive industry give the net excess oxygen in the flue gas, *i.e.* the AFR. Therefore, we can compute the FAER from the output of the Lambda sensor. In an experimental study on air gasification of polypropylene, Xiao *et al.* [12] studied the effect of the ER and found that equivalence ratio appeared to have a significant effect on the reactor temperature and other gasification results. The increase of the equivalence ratio favored the formation of the fuel gas and decreased the formation of the tars and char. Other authors obtained similar results [13] [14] [15]. Summarizing is the work done by Vaezi *et al.* [16] who used the thermochemical equilibrium modeling to predict the performance of a heavy fuel oil gasifier. Their model combined both the chemical and thermodynamic equilibriums of the global gasification reaction in order to predict the final syngas species distribution. They compared the results of their simulations with reported experimental measurements through which their numerical model was validated. They found that the optimum value of ER respective to producer gas yield was around 0.35.

Therefore, monitoring of the ER is a good parameter for controlling the gasification process of biomass. We have designed, fabricated, and tested two charcoal and wood-fired downdraft biomass gasifiers in Burkina Faso [17]. Unfortunately, we were limited by the failure of the five flue gas analyzers we have on hand and even the replacement of the oxygen or carbon monoxide sensors appeared out of reach, because these are relatively costly and not suited for long-run usage (maximum 5 minutes of continues use recommended by the manufacturers). We therefore seek replacement solutions to that problem and found that several authors used Lambda sensors to monitor the excess air and other gases like carbon monoxide, hydrogen, and methane sensors in industrial applications [18] [19] [20].

As claimed by Lambda sensors makers [21], these probes have the following advantages over other existing methods of measuring oxygen concentration in our context:

- Resistant to corrosion by acid and aggressive substances.

- The sensor can be placed directly in the exhaust gas flow.
- Lambda sensor can be used in the analysis of wet gases, since it operates at a high temperature where no condensation could occur.
- Cleaning, cooling and drying of a gas sample for analysis is not necessary.
- The cell output signal increases with the decrease of the oxygen concentration in the analyzed gas.

We also found that microcontrollers can be used to acquire data from numerous sensors, compute several mathematical functions and display or log these values in an USB drive [22] [23] [24] [25] [26]. Arduino appeared to us as the most beginners friendly and we opted for it.

Using Lambda sensors and the Arduino microcontroller emerged as a very interesting and cost-effective replacement solution for monitoring the ER in our biomass gasifiers.

## 2. Materials and Methods

### 2.1. Experimental Setup

The downdraft wood gasifier used in this work is a co-current gasifier also known as Imbert Gasifier. A K type a Lambda sensor have been fixed after the reduction zone, where gaseous products consist of the producer gas ( $\text{CO} + \text{H}_2 + \text{CH}_4$ ) which are combustibles and non-combustibles gases like nitrogen ( $\text{N}_2$ ), carbon dioxide ( $\text{CO}_2$ ) and water vapor ( $\text{H}_2\text{O}$ ). A nominal 12 V rated air blower feed the gasifier with the required amount of air. The microcontroller used to drive our system is an Arduino Uno 3. Overview of the experimental setup is given on **Figure 1** below.

Arduino is a development board that can be programmed using an Integrated Development Environment (IDE) written in C++ called Arduino IDE. Arduino Uno 3 board we are using in this work has six analog input pins labeled A0 to A5 and fourteen digital pins labeled D0 to D13. Pins D3, D5, D6, D9, D10 and D11

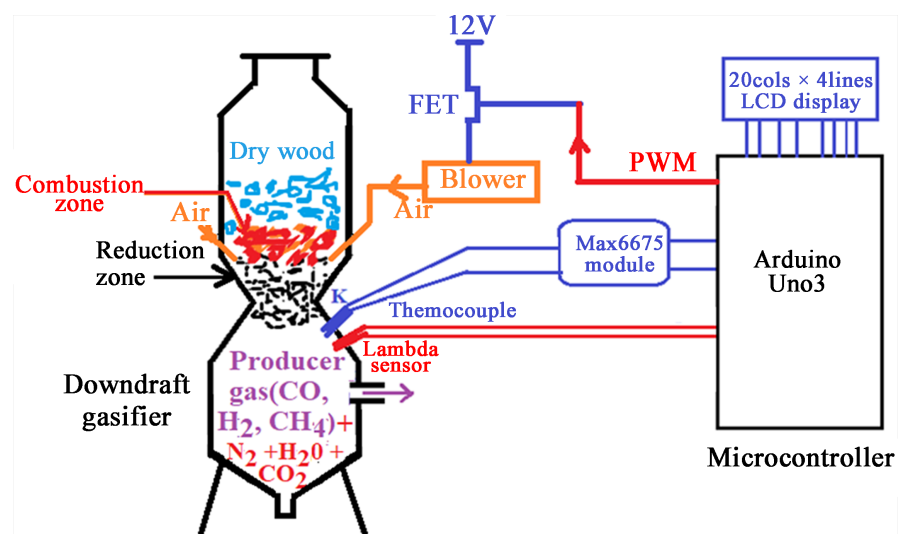


**Figure 1.** Experimental setup.

can also use Pulse Wide Modulation (PWM). Technical specifications of the Arduino Uno 3 development board are given in **Table 1** below:

## 2.2. Methods

### 2.2.1. Determination of the Temperature

A K type thermocouple is used along with its amplification and analog to digital converter referenced as Max6675 to acquire the working temperature of the gasifier in °C where the Lambda sensor is plugged in.

The MAX6675 can measure temperatures from 0°C to +1024°C, performs cold-junction compensation and digitizes the signal from a type-K thermocouple. The data is output in a 12-bit resolution, serial peripheral interface (SPI) compatible, read-only format. On **Figure 2** below, the Max6675:

- Processes the reading from the thermocouple and transmits the data through a serial interface.
- Force CS low and apply a clock signal at SCK to read the results at SO. Forcing CS low immediately stops any conversion process.
- Initiate a new conversion process by forcing CS high.
- Force CS low to output the first bit on the SO pin.

That way, Max6675 gives us a compensated temperature reading from ambient temperature to the working temperature of the Lambda sensor. Conversion in K is made in the Arduino Integrated Development Environment (IDE).

**Table 1.** Arduino Uno 3 technical specifications.

Microcontroller	ATmega328P
Operating Voltage	5 V
Input Voltage (recommended)	7 - 12 V
Input Voltage (limit)	6 - 20 V
Digital I/O Pins	14 (of which 6 provide PWM output)
PWM Digital I/O Pins	6
Analog Input Pins	6
DC Current per I/O Pin	20 mA
DC Current for 3.3 V Pin	50 mA
Flash Memory	32 KB (ATmega328P) of which 0.5 KB used by bootloader
SRAM	2 KB (ATmega328P)
EEPROM	1 KB (ATmega328P)
Clock Speed	16 MHz
LED_BUILTIN	13
Length	68.6 mm
Width	53.4 mm
Weight	25 g

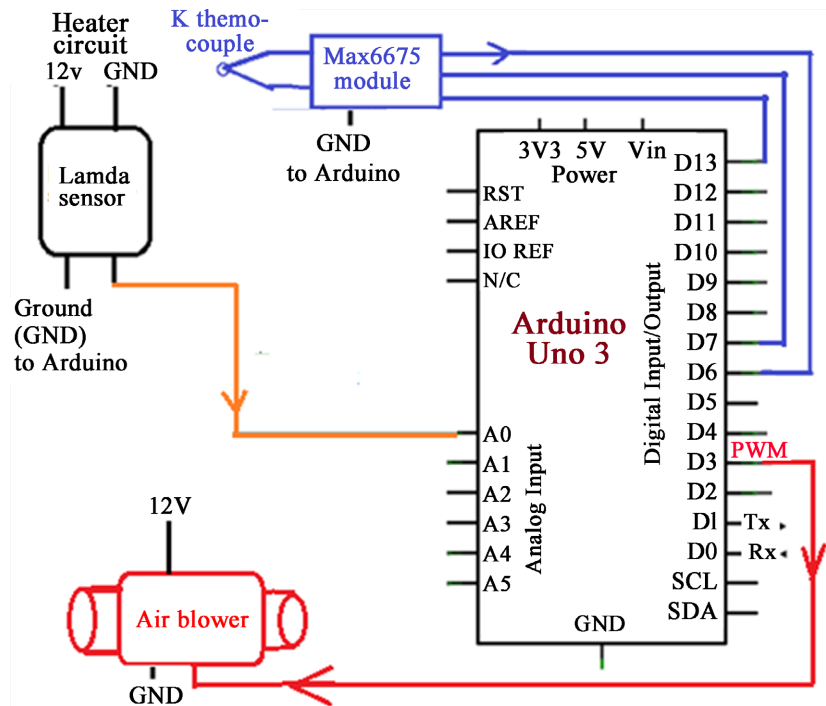


Figure 2. Overall diagram of the monitoring system.

The Max6675 outputs a digital value of the temperature on pin DO. That value is read on seventh digital pin D6 of the microcontroller and can be used for calculations.

### 2.2.2. Determination of the Oxygen Concentration

A zirconium oxide oxygen sensor, as for example the commercial narrowband Lambda sensor used in the automotive industry, consists of a pair of porous platinum electrodes separated by a layer of the zirconium oxide.

Working principle of the zirconia probe described below is inspired from OxyPink [21]. It is an electrochemical galvanic cell comprising of two electrically conducting, chemically inert. A zirconia cell, is a kind of solid electrolyte, it is coated on the outside (measuring electrode) and inside (reference electrode) with a thin porous layer of metal, generally platinum as illustrated on Figure 2 below.

At temperatures above 600°C, zirconium oxide becomes an Oxygen ion conductor, which generates an Electromotive Force (EMF) between the platinum electrodes. This EMF depends on the difference between the partial pressure of oxygen in the sample gas and the Oxygen in the reference gas (using ambient air).

Two different ion concentrations on either side of an electrolyte generate an electrical potential known as the Nernst voltage. The larger the difference in the ion concentration ratio, the greater the voltage. Above 600°C zirconium dioxide ( $ZrO_2$ ) exhibits two mechanisms:

- $ZrO_2$  partly dissociates to produce oxygen ions which can be transported through the material when a voltage is applied.

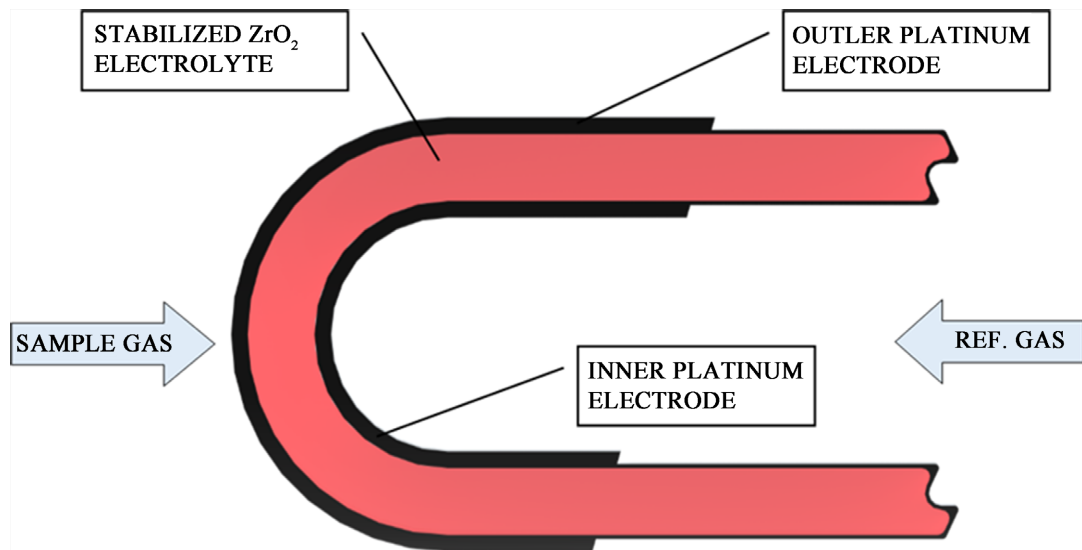


**Figure 3.** Working priciple of Lambda sensors from [19].

- $ZrO_2$  behaves like a solid electrolyte for oxygen. If two different oxygen pressures exist on either side of an  $ZrO_2$  element a voltage (Nernst voltage) can be measured across that element.

Molecular oxygen is ionized at the porous platinum electrodes according to Equations (1) and (2) below:



The platinum electrodes on each side of the cell provide a catalytic surface for the change in oxygen molecules ( $O_2$  to oxygen ions), and oxygen ions to oxygen molecules. Oxygen molecules on the high concentration reference gas side of the cell gain electrons to become ions which enter the electrolyte. Simultaneously, at the other electrode, oxygen ions lose electrons and are released from the surface of the electrode as oxygen molecules. The oxygen content of these gases, and therefore the oxygen partial pressures, is different. Therefore, the rate at which oxygen ions are produced and enter the zirconium oxide electrolyte at each electrode differs. As the zirconium oxide permits mobility of oxygen ions, the number of ions moving in each direction across the electrolyte will depend on the rate at which oxygen is ionized and enters the electrolyte at each electrode. The mechanism of this ion transfer is complex, but it is known to involve vacancies in the zirconia oxide lattice by doping with yttrium oxide. The result of migration of oxygen ions across the electrolyte is a net flow of ions in one direction depending upon the partial pressures of oxygen at the two electrodes.  $P_1$  denoting partial pressure of the reference gas (outside air) and  $P_2$  the partial pressure of the sampling gas and EMF the resulting electro-motive force:

- If  $P_1 > P_2$  ions flows from  $P_1$  side to  $P_2$  side which give a positive EMF.

- If  $P_1 < P_2$  ions flows from  $P_2$  side to  $P_1$  side which give a negative EMF.
- If  $P_1 = P_2$  there is no net ions flow. This result in a zero EMF.

This behavior is summarized on figure below:

For the gasification application, when working in sub-stoichiometric conditions, *i.e.* with excess fuel, EMF of the Lambda sensor should therefore between 200 mV and 800 mV for excess fuel between 0 and 15% according to **Figure 3** above.

The EMF ( $E$ ) developed by the zirconium probe is called *Nernst Voltage* and is related to partial pressures  $P_1$  and  $P_2$  through an equation called *Nernst Equation* that can be derived from the Gibbs free energy under standard conditions as follow:

$$E^0 = E_{reduction}^0 - E_{oxydation}^0 \tag{3}$$

Variation of Gibbs free energy  $\Delta G$  is also related to E under general conditions as:

$$\Delta G = -nFE \tag{4}$$

where:

- $n$  is the number of electrons transferred in the reaction (from balanced reaction),
- $F$  is the Faraday constant (96,500 C/mol), and
- $E$  is potential difference.

Under standard conditions, Equation (4) is then

$$\Delta G_0 = -nFE_0 \tag{5}$$

From thermodynamics, the Gibbs energy change under non-standard conditions can be related to the Gibbs energy change under standard Equations via

$$\Delta G - \Delta G_0 = nRT \ln(Q) \tag{6}$$

Substituting  $\Delta G = -nFE$  and  $\Delta G_0 = -nFE_0$  into Equation (6), we have:

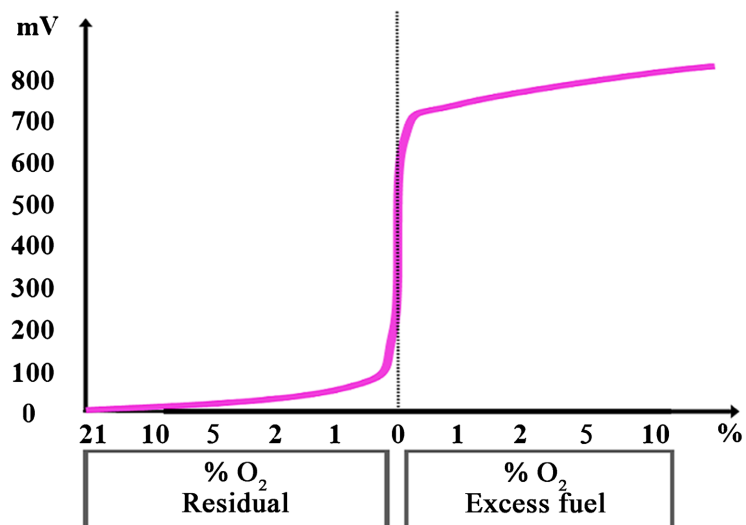


**Figure 4.** Zirconium Lambda sensor EMF relation to oxygen content [19].

$$-nFE + nFE_0 = RT \ln(Q) \quad (7)$$

Dividing both sides of the Equation above by  $-nF$ , and rearranging terms we have:

$$E - E_0 = -nRTF \ln(Q) \quad (8)$$

Analog signal from the Lambda sensor was directed to analog input  $A_0$  pin of the Arduino Uno 3 board as illustrated on **Figure 2** above. From Equation (8), Oxygen concentration is then determined through the Nernst Law:

$$O_2 (\%) = 20.96 \exp\left(-\frac{zF}{RT}(E - E_0)\right) \quad (9)$$

20.96 is the volumic concentration of oxygen in clean air,

$z$  is the number of electrons migrating between the sensor electrodes,

$F$  is the Faraday constant,

$E$  is the amplified voltage developed across the sensor terminals,

$R$  is the universal constant of ideal gases,

$T$  is the absolute temperature in the Lambda sensor.

A commercial heated 4 wires Lambda sensor was installed in the reduction zone of a downdraft gasifier. Close to the Lambda sensor was installed a type K thermocouple. A simple, electrical circuit comprising a 12V DC power source in serial with an ampere meter and the heating element of the Lambda sensor was used. An electronic voltmeter was attached in parallel to the heating element. An oscilloscope was also attached to the signal wires of the Lambda sensor to monitor output signal from the Lambda sensor.

### 2.2.3. Determination of the Equivalence-Ratio (ER)

For biomass gasification, the equivalence ratio (ER) of a system is defined as the ratio of the hydrocarbon-to-oxidizer ratio to the stoichiometric hydrocarbon-to-oxidizer ratio which can be expressed with Equation (10) below:

$$FAER = \frac{(fuel\ to\ oxidizer\ ratio)_{real}}{(fuel\ to\ oxidizer\ ratio)_{stoich}} = \frac{(m_{fuel}/m_{oxy})_{real}}{(m_{fuel}/m_{oxy})_{stoich}} = \frac{FAR_{real}}{FAR_{stoich}} \quad (10)$$

In Equation (1),  $m$  represents the mass,  $n$  represents number of moles. Subscripts *real* and *stoich* refer to real and stoichiometric ratios respectively for the corresponding mass or mole fractions. According to Vaclav *et al.* [27]: if air is used as the oxidizer, Equation (10) can be rewritten as follow:

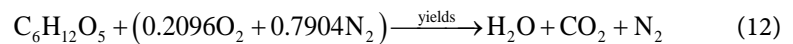
$$FAER = \frac{(fuel\ to\ oxidizer\ ratio)_{real}}{(fuel\ to\ oxidizer\ ratio)_{stoich}} = \frac{(m_{fuel}/m_{air})_{real}}{(m_{fuel}/m_{air})_{stoich}} \quad (11)$$

ER is calculated using Equation (11), *i.e.*, we are considering FAR and FAER. We must first find the stoichiometric FAR of wood in clean air. Wood composition slightly varies between species, but can be in first approximation represented as  $C_6H_{12}O_5$ , when wood is supposed not to contain nitrogen or minerals.

Equation of stoichiometric combustion of wood in air containing 20.96% of

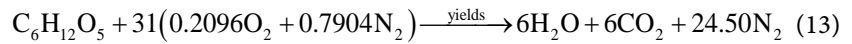


oxygen and 79.04% of nitrogen is the following:



Chemical species conservation allows us to calculate  $\alpha$ ,  $\beta$ ,  $\gamma$  and  $\varepsilon$ .

Then:



Equation (13) above teach us that stoichiometric combustion of 1 mole of wood having a mass of  $M_{air} = 6 * 12 \text{ g} + 12 * 1 \text{ g} + 5 * 16 \text{ g} = 164 \text{ g}$ , would require:

$31 * (0.2096 * 16 \text{ g} * 2 + 0.7904 * 14 \text{ g} * 2) = 31 * 28.8384 \text{ g} = 31M_{air} = 893.9904 \text{ g}$  of air, which represents 31 “moles” of air.

Therefore:

$$FAR_{stoich} = \left( \frac{m_{fuel}}{m_{air}} \right)_{stoich} = \frac{164 \text{ g}}{893.9904 \text{ g}} = 0.1834472 \quad (14)$$

Under sub-stoichiometric conditions of the gasification  $\alpha$  (less than 31) is the actual number of “moles” of air that is used. Therefore:

$$FAR_{real} = \left( \frac{m_{fuel}}{m_{air}} \right)_{real} = \frac{1}{AFR_{real}}$$

Lambda sensors display the net AFR., ie 1/FAR. Therefore:

$$\phi = FAER = \frac{1}{AFER} = \frac{1}{\lambda} = \frac{FAR_{real}}{FAR_{stoich}} = FAR_{real} * \frac{1}{FAR_{stoich}}$$

Taking in account value of Equation (14), we finally have:

$$FAER_{real} = \frac{1}{\lambda} = \frac{FAR_{real}}{FAR_{stoich}} = \frac{5.4512}{AFR_{real}} \quad (15)$$

### 3. Results and Discussion

In order to calculate the oxygen percentage in flue gas, we need the working temperature of the lambda sensor and the EMF developed by that sensor. Therefore, we must first find these values with Arduino UNO 3. In C++, // denote a comment.

#### 3.1. Measurement of the Temperature

The following lines of C++ code were used for calculating the temperature within Arduino UNO 3:

```
#include <LiquidCrystal.h>
#include "max6675.h"
LiquidCrystal lcd(12,8,13,4,3,2); //Setup the LCD
int thermoDO = 7; //Pin used by DO
int thermoCS = A5; //pin Used for CS
```

```
int thermoCLK = 6; //Clock pin to 6
float temperature = 0.0; //Define temperature
void setup()
    {
    Serial.begin(9600);
    lcd.begin(20,4); //set the LCD's number of columns and rows
    } ; //End Setup

void loop()
    {
    temperature = thermocouple.readCelsius()+273.15;
    To2=temperature; //Temperature is calculated in K
    lcd.clear(); // Clear LCD to avoid weird characters display
    lcd.setCursor(0,0); // Put the LCD cursor
    //at column 1 of line 1.
    lcd.print("T ");
    lcd.print(temperature-273.15,1); //Display
    //Reactor temperature in °C with 1 decimal
    lcd.print((char)223); //
    lcd.print("C or ");
    lcd.setCursor(12,0); //Go to column 13 of line 1.
    lcd.print(temperature,1); //Display temperature in K
    //with 1 decimal
    lcd.print(" K");
    delay(30000); // Wait 30 seconds.
    } //End loop
```

### 3.2. Calculation of the EMF Developed by the Lambda Sensor and Oxygen Percentage

The following lines of code were used for calculating the oxygen percentage with Arduino. These take place in the same sections of the program as that the temperature. In fact, there is only one “loop” statement in the program:

```
int OxyPin = A0; // Oxygen pin set to A0
int vccPin = 3; //Vcc pin of 5V is pin 3
int gndPin = 2; //Ground is pin 2
//Declarations before calculating Oxygen
float oxyPercent; //Define oxygen as a real number
float eO2=0.0; //Analog voltage developed by the lambda sensor
float To2=600.0; //Working temperature of the lambda sensor
#define F 96485.34 //Define the Faraday constant
#define R 8.314 // Define the constant gases
#define O2Air 20.9 //Define Oxygen concentration in clean air
#define T0 273.2 // Define T0 temperature in K
```

```

#define Coef 1.025 //Correction coefficient for calibration
#define z 1.125*pow(10,-5) //Number of electron migrating
long unsigned intervalHigh = 30000; // 30 seconds of
//measurements interval
float Tom = 0.0; //Declare time of measure as a real number
float tempCels = 0.0; //Define temperature in Celsius
// as a real number
void loop() //This the same loop as for
{ //temperature above. Not another.
tempCels = temperature - 273.15; //Temperature in Celsius
//Oxygen with Lambda sensor
eO2 = analogRead(OxyPin); //Pin where O2 emf is to be read
oxyPercent = Coef*O2Air*exp(-(z*F*eO2)/(R*To2));
// Calculate Oxygen concentration according to
//equation derived from the Nernst Law
//Display O2 in %
lcd.setCursor(0,1); //Set LCD cursor at line 2, column 1
lcd.print("O2 ");
lcd.print(oxyPercent, 2); // Print Oxygen content on LCD
lcd.print(" %");
lcd.setCursor(0,3); //Set LCD cursor at line 4, column 1
lcd.print("emf ");
lcd.print(eO2,1); //Display value of the emf
} //End loop. The same loop as for temperature above.

```

### 3.3. Calibration of the Lambda Sensor

The Lambda sensor doesn't require a complicated or costly calibration, but the heater resistance of a Lambda sensor vary from a supplier to another. We thus first check the response of the heating element during the application of a continuous electrical power aiming to set the required working temperature of the Lambda sensor to more than 600°C as required by manufacturers.

Heating the Lambda sensor is necessary in order to put the sensing ZnO<sub>2</sub> porous film in conducting state. We must also check that the Lambda sensor is working as intended.

**Figure 5** below show variation of the current flowing through the Lambda sensor and the heating element resistance when subjected to a 12 V DC power from a solar battery.

We can see in **Figure 5** above that the resistance of our Lambda sensor augment from 14.6Ω at 30 seconds of heating to 25.1Ω at 10 minutes and is then stabilized.

### 3.4. Computing the FAER

Code for calculating the FAER written in C++ within the Arduino 2.2.1 IDE is given below.

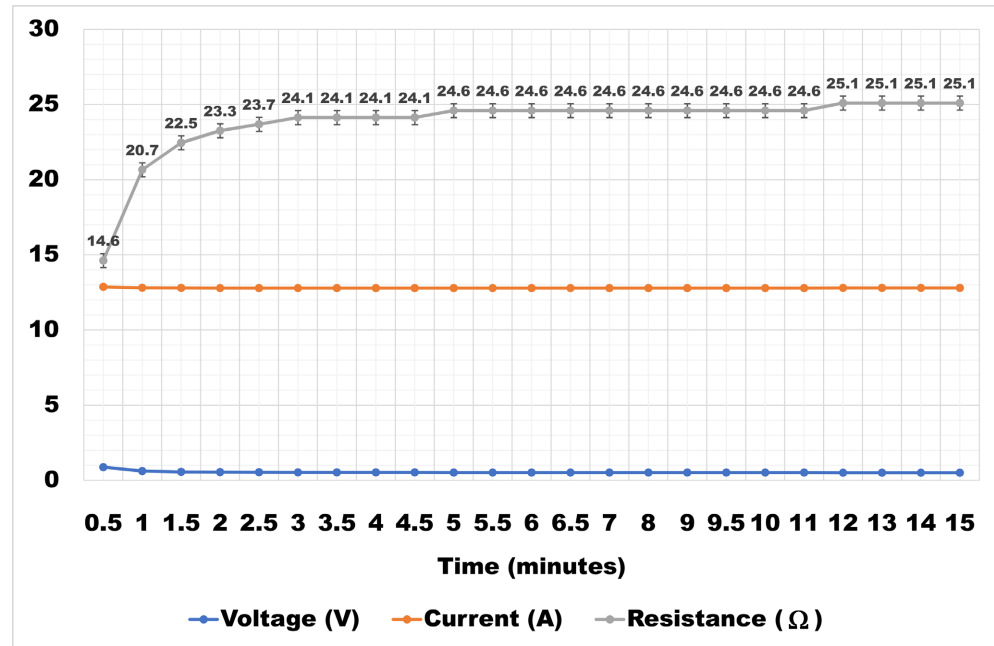


Figure 5. Variation of the resistance of the heating element inside the Lambda sensor during the application of an 12V DC solar battery power supply.

```
float afr = 0.0; //Define afr as a real number
float FAER = 0.0; //Define FAER as a real number
void loop() //This the same loop as for
{
  //temperature above. Not another.
  afr = 0.1865*oxyPercent; //Calculate AFR from oxygen %
  FAER = 5.4512/afr ;//Calculate FAER according to equation 15
  lcd.setCursor(11,1); //Put LCD cursor to line 2, column 12
  lcd.print("AFR ");
  lcd.print(afr, 2); //Display AFR with 2 decimals
  lcd.setCursor(16,1); //Put LCD cursor to line 2, column 17
  lcd.print("FAER ");
  lcd.print(afr, 2); //Display FAER with 2 decimals
  //Display what is the time elapsed?
  lcd.setCursor(0,2); //Set LCD cursor at line 3, column 1
  lcd.print("Meas. time ");
  unsigned long currentMillis = millis(); //Millis is an
  //internal function of Arduino giving time in milliseconds
  //elapsed since the latest power up of the board
  Tom = ((currentMillis/1000)/60.0); //Calculate time of
  //measure in minutes
  lcd.setCursor(11,2); //Put LCD cursor to line 3, column 12
  lcd.print(Tom,1); //Display time of measure
  lcd.print(" min");
} //End loop. The same loop as for temperature above.
```

### 3.5. Costs Estimation

We set aside work time because this work is done as a regularly paid physicist. The prices of the materials used for this project are as follows:

- Arduino Uno 3 starter kit:	\$34
- Max6675 thermocouple module:	\$7
- 2x Lambda sensor:	\$25
- 10x PCB prototyping boards:	\$7
- Shipping fees:	\$65
- Duty fees:	\$100

-----  
Total cost: \$238

Cost of a commercial oxygen analyzer is about \$1750 in Burkina Faso.

### 3.6. Discussion

According to the Max6675 datasheet, values of temperature have resolution of  $0.25^{\circ}\text{C}$  and an accuracy of  $\pm 1.5^{\circ}\text{C}$ . That is enough for our application in gasification where temperatures range from ambient  $25^{\circ}\text{C}$  to gasification temperatures of up  $1200^{\circ}\text{C}$ .

The Lambda sensor first showed an alternating voltage in the order of 20 mV on the digital oscilloscope when not heated and an almost constant voltage of 80 mV after 15 minutes of heating. This reminds us of the importance of the heater in the Lambda sensor. Calculation of the residual oxygen concentration in the flue gas only requires the mastering of the Arduino programming, which is C++. However, by using the Arduino Uno 3 starter kit, things become easier, and physicists like us, who have already faced programming by their function, such as with MATLAB should, with a little effort, do likewise.

Results obtained are displayed on a 20 columns with 4 lines LCD display as see in **Figure 6** below:

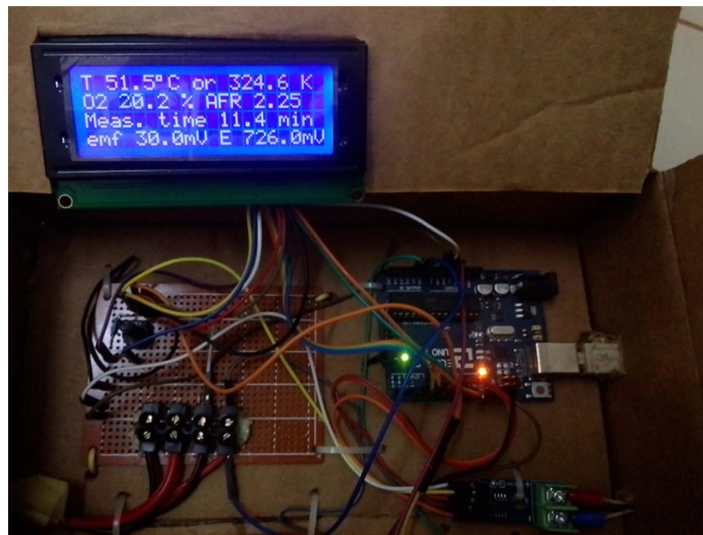


**Figure 6.** Finished prototype with LCD display.

## 4. Conclusion

We have designed and manufactured an equivalence ratio monitoring system driven by an Arduino Uno 3 board. The temperature is recorded with an accuracy of  $\pm 1.5^{\circ}\text{C}$ . After the 10-minute heating time has elapsed, the response time to the measured temperature change is approximately 3 s. This is sufficient for the use we make of this monitoring system in our project. Lambda oxygen sensors can operate without problems at the high temperatures found in gasifiers. This is one of the reasons why they are widely used in automobiles to control the fuel injection of internal combustion engines. Additionally, Lambda sensors last for years before needing replacement and require very little maintenance. They can operate without problems in contact with exhaust fumes, provided that humidity in these fumes is avoided. Making this device helped us overcome the difficulties we faced during our gasification experiments. This affordable oxygen monitoring system only cost us a seventh part of the price of a new oxygen analyzer in Burkina Faso. With the need and scarcity of C++ programming skills, researchers in developing countries can take advantage of this system where it may be difficult to have oxygen displacement systems.

## Conflicts of Interest

The authors declare no conflicts of interest regarding the publication of this paper.

## References

- [1] Sustainable Energy for All (2023) [Burkina Faso]: Rapid Assessment and Gap Analysis.  
[https://www.seforall.org/sites/default/files/Burkina\\_Faso\\_RAGA\\_FR\\_Released.pdf](https://www.seforall.org/sites/default/files/Burkina_Faso_RAGA_FR_Released.pdf)
- [2] Nyika, J., Adesoji Adediran, A., Olayanju, A., Adesina, O.S. and Edoziuno, F.O. (2020) The Potential of Biomass in Africa and the Debate on Its Carbon Neutrality. In: Basso, T.P., Basso, T.O. and Basso, L.C., Eds., *Biotechnological Applications of Biomass*, IntechOpen Limited, London.
- [3] Fidele, N.J., Jean, K. and Gérard, S.B. (2014) Potential and Feasibility of Solid Municipal Waste Treatment with Gasifiers in a Developing Country: A Review for Burkina Faso. *British Journal of Applied Science & Technology*, **4**, 450-464.  
<https://www.sciencedomain.org/>  
<https://doi.org/10.9734/BJAST/2014/6853>
- [4] Wood-Based Biomass Energy Development for Sub-Saharan Africa: Issues and Approaches.  
<https://openknowledge.worldbank.org/entities/publication/9bb75b9a-7102-513b-99be-4895fbff7e2f>  
<http://hdl.handle.net/10986/26149>
- [5] VENRO (2009) Rethinking Biomass Energy in Sub-Sahara Africa,  
[https://venro.org/fileadmin/user\\_upload/Dateien/Daten/Publikationen/Factsheets/009\\_Afrika\\_EU\\_Bioenergiestudie\\_englisch.pdf](https://venro.org/fileadmin/user_upload/Dateien/Daten/Publikationen/Factsheets/009_Afrika_EU_Bioenergiestudie_englisch.pdf)
- [6] Petrie, B. and Macqueen, D.J. (2013) South African Biomass Energy: Little Heeded But Much Needed.  
<https://www.iied.org/sites/default/files/pdfs/migrate/17165IIED.pdf>

- [7] Jangsawang, W., Laohalidanond, K. and Kerdsuwan, S. (2015) Optimum Equivalence Ratio of Biomass Gasification Process Based on Thermodynamic Equilibrium Model. *Energy Procedia*, **79**, 520-527. <https://doi.org/10.1016/j.egypro.2015.11.528>
- [8] Salaudeen, S.A., Arku, P. and Dutta, A. (2019) Chapter 10—Gasification of Plastic Solid Waste and Competitive Technologies. In: Al-Salem, S.M., Ed., *Plastics to Energy: Fuel, Chemicals, and Sustainability Implications*, William Andrew, Norwich, 269-293. <https://doi.org/10.1016/B978-0-12-813140-4.00010-8>
- [9] Arena, U. (2013) Chapter 17, Fluidized Bed Gasification. In: Scala, F., Ed., *Fluidized Bed Technologies for Near-Zero Emission: Combustion and Gasification*, William Andrew, Norwich, 765-812. <https://doi.org/10.1533/9780857098801.3.765>  
<https://www.sciencedirect.com/science/article/pii/B9780857095411500170>
- [10] Reed, T.B. and Das, A. (1950) Handbook of Biomass Downdraft Gasifier Engine Systems. Solar Energy Research Institute, Selangor. <https://www.nrel.gov/docs/legosti/old/3022.pdf>
- [11] Bukar, A.A., Oumarou, M.B., Tela, B.M. and Eljummah, A.M. (2019) Assessment of Biomass Gasification: A Review of Basic Design Considerations. *American Journal of Energy Research*, **7**, 1-14.
- [12] Xiao, R. and Jin, B.S. (2007) Air Gasification of Polypropylene Plastic Waste in Fluidized Bed Gasifier. *Energy Conversion and Management*, **48**, 778-786. <https://doi.org/10.1016/j.enconman.2006.09.004>
- [13] Saleha, S. and Samad, N.A.F.A. (2021) Effects of Gasification Temperature and Equivalence Ratio on Gasification Performance and Tar Generation of Air Fluidized Bed Gasification Using Raw and Torrefied Empty Fruit Bunch. *Chemical Engineering Transactions*, **88**, 1309-1314. <http://www.cetjournal.it/cet/21/88/218.pdf>
- [14] Kumar, M., Paul, B. and Yadav, D.S. (2016) Effect of Moisture Content Andequivalence Ratio on The Gasificationprocess for Different Biomass Fuel. *International Journal of Mechanical Engineering and Technology (IJMET)*, **7**, 209-220. <http://iaeme.com/Home/issue/IJMET?Volume=7&Issue=6>
- [15] Sidek, F.N., Abdul Samad, N.A.F and Saleh, S. (2020) Review on Effects of Gasifying Agents, Temperature and Equivalence Ratio in Biomass Gasification Process. *IOP Conference Series: Materials Science and Engineering*, Kuantan, 1-2 October 2019, Article ID: 012028. <https://doi.org/10.1088/1757-899X/863/1/012028>
- [16] Vaezi, M., Passandideh-Fard, M., Moghiman, M. and Charmchi, M. (2010) Gasification of Heavy Fuel Oils: A Thermochemical Equilibrium Approach. *Fuel*, **90**, 878-885. <https://doi.org/10.1016/j.fuel.2010.10.011>
- [17] Fidele, N.J., Salou, H., Kossi, I., Gerard, S.B., Frederic, O. and Hamadou, T. (2023) Electrical Power Generation from Heat Recovered at the Throat of a Downdraft Biomass Gasifier. *American Journal of Science, Engineering and Technology*, **8**, 133-140. <http://www.sciencepublishinggroup.com/j/ajset>  
<https://doi.org/10.11648/j.ajset.20230803.12>
- [18] de Souza Sobrinho, A.S., Cavalcante Junior, F.S. and de Lima, L.C. (2012) Monitoring Industrial Combustion through Automotive Oxygen Sensor. *International Transaction Journal of Engineering, Management, & Applied Sciences & Technologies*, **3**, 203-211. <http://TuEngr.com/V03/203-211.pdf>
- [19] Aravind, S., Ragupathi, P., Sathish Kumar, D. and Vignesh, G. (2020) A Numerical Investigation of Automotive Lambda Sensor to Improve the Life Span of the Sensor Using CFD. *IOP Conferences Series: Materials Science and Engineering*, **923**, Article ID: 012003. <https://doi.org/10.1088/1757-899X/923/1/012003>
- [20] Brailsford, A.D., Yussouff, M., Logothetis, E.M. and Shane, M. (1995) Steady-State

- Model of a Zirconia Oxygen Sensor in a Simple Gas Mixture. *Sensors and Actuators B: Chemical*, **25**, 362-365. [https://doi.org/10.1016/0925-4005\(95\)85081-3](https://doi.org/10.1016/0925-4005(95)85081-3)
- [21] OxyPink (2023) Zirconia Oxygen Probe. <https://oxypink.com/en/zirconia-oxygen-probe/>
- [22] Nasir, A.Y., Bature, U.I., Tahir, N.M., Babawuro, A.Y., Boniface, A. and Hassan, A.M. (2020) Arduino Based Gas Leakage Control and Temperature Monitoring System. *International Journal of Informatics and Communication Technology*, **9**, 171-178. <https://doi.org/10.11591/ijict.v9i3.pp171-178>
- [23] Ahmed, S. (2016) Intelligent Bio-Detector. *Open Journal of Applied Sciences*, **6**, 903-937. <https://doi.org/10.4236/ojapps.2016.613078>
- [24] Nasir, A.Y., Bature, U.I., Tahir, N.M., Babawuro, A.Y., Boniface, A. and Hassan, A.M. (2020) Arduino Based Gas Leakage Control and Temperature Monitoring System. *International Journal of Informatics and Communication Technology*, **9**, 171-178. <http://ijict.iaescore.com>  
<https://doi.org/10.11591/ijict.v9i3.pp171-178>
- [25] Yan, H.H. and Rahayu, Y. (2014) Design and Development of Gas Leakage Monitoring System Using Arduino and ZigBee. *Proceeding of International Conference on Electrical Engineering, Computer Science and Informatics (EECSI 2014)*, Yogyakarta, 20-21 August 2014, 207-212.
- [26] Dewi, L. and Somantri, Y. (2018) Wireless Sensor Network on LPG Gas Leak Detection and Automatic Gas Regulator System Using Arduino. *IOP Conference Series: Materials Science and Engineering*, **384**, Article ID: 012064. <https://doi.org/10.1088/1757-899X/384/1/012064>
- [27] Nevrlý, V., Dostál, M. and Zelinger, Z. (2022) Ultra-Lean Combustion Mode in Fundamentals of Low Emission Flameless Combustion and Its Applications. Academic Press, Cambridge, 13-43. <https://doi.org/10.1016/C2020-0-02292-9>